

# Viscous fingering of a miscible reactive $A+B\rightarrow C$ interface for an infinitely fast chemical reaction: Nonlinear simulations

Y. Nagatsu<sup>1,2</sup> and A. De Wit<sup>2</sup>

<sup>1</sup>Department of Materials Science and Engineering, Graduate School of Engineering, Nagoya Institute of Technology, Gokiso-cho, Showa-ku, Nagoya, Aichi 466-8555, Japan

<sup>2</sup>Nonlinear Physical Chemistry Unit, Service de Chimie Physique et Biologie Théorique, Université Libre de Bruxelles (ULB), CP 231, Faculté des Sciences, Campus Plaine, 1050 Brussels, Belgium

(Received 9 February 2011; accepted 25 February 2011; published online 18 April 2011)

Nonlinear dynamics of miscible viscous fingering is analyzed numerically for a reactive system when a solution containing a reactant  $A$  is displacing another miscible solution containing another reactant  $B$ . A simple  $A+B\rightarrow C$  reaction takes place upon contact of the solutions. The viscosity of the fluid depends on the concentration of the various chemicals. The nonlinear fingering dynamics is studied numerically for an infinite Damköhler number  $D_a$ , i.e., for an infinitely fast reaction as a function of the log-mobility ratios  $R_b$  and  $R_c$  quantifying the viscosity ratios of the solutions of  $B$  and  $C$ , respectively, versus that of the solution of  $A$ . If  $R_b > 0$ , i.e., if the system is genuinely viscously unstable because the displacing solution of  $A$  is less viscous than the displaced solution of  $B$ , we analyze the changes to classical nonreactive viscous fingering induced by the reaction. If on the contrary  $R_b < 0$ , which corresponds to a hydrodynamically stable case in absence of reactions, we study chemically driven viscous fingering occurring when the chemical reaction triggers a nonmonotonic viscosity profile. Comparison between the present simulation results and corresponding linear stability analysis and experiments is also conducted. © 2011 American Institute of Physics. [doi:10.1063/1.3567176]

## I. INTRODUCTION

Viscous fingering (VF) is a hydrodynamic instability occurring when a less viscous fluid is displacing another more viscous one in a porous medium.<sup>1</sup> The interface between the two fluids becomes unstable and forms a finger-like pattern. Recently, coupling between viscous fingering and chemical reactions has been investigated both experimentally and theoretically. The related studies can be classified into two categories depending on whether chemical reactions are passive or active to fluid motion. In the passive cases (i.e., when the chemical species are simply advected by the flow), attention has been paid to analyze concentration distributions of the chemicals advected by fingering. The patterns observed depend on the initial concentrations and on the fingering velocity.<sup>2-6</sup> In the active cases, the reaction modifies the fluid motions by changing a physical property of the solution like viscosity, permeability, or surface tension for instance. The fingering pattern can directly be affected by those chemically driven changes. Experiments have evidenced for example changes in the fingering pattern due to a decrease in interfacial tension induced by a reaction in immiscible systems<sup>7</sup> or due to an increase in permeability by a precipitation reaction in miscible systems.<sup>8</sup>

In miscible systems, changes in the fluid viscosity due to reactions have also been shown to influence viscous fingering patterns. Nagatsu *et al.* have recently performed experimental studies of such reactive viscous fingering in miscible systems in a Hele–Shaw cell.<sup>9,10</sup> A simple  $A+B\rightarrow C$  chemical reaction takes place when a reactive solution of  $A$  displaces a more viscous solution of  $B$  producing the product  $C$  at the interface. The fluid viscosity depends on the concen-

trations of species  $B$  and  $C$  only. Two different situations were analyzed depending on the value of the Damköhler number  $D_a$  defined as the ratio between the characteristic time of fluid motions and that of the chemical reaction. In Nagatsu *et al.*, it was found that, for fast reactions (large  $D_a$ ), shielding was suppressed, and hence the fingering pattern became more dense within a given area when the product  $C$  is more viscous than the reactant  $B$ .<sup>9</sup> Reverse effects were obtained for reactions generating a less viscous product  $C$ . Other experiments by Nagatsu *et al.* have investigated slower reactions, i.e., moderate  $D_a$  conditions in the same case where the product is less viscous than the reactant of  $B$ .<sup>10</sup> It was shown that the fingering pattern is denser in the reactive case than in the nonreactive case. This finding, interestingly, showed that opposite dynamical tendencies can be obtained with reactions both decreasing the viscosity for moderate  $D_a$  or high  $D_a$ , respectively.

In these experiments by Nagatsu *et al.*,<sup>9,10</sup> the displacing solution  $A$  is less viscous than the invaded solution of  $B$  so that the system is genuinely viscously unstable even without any reaction. The chemically driven changes in viscosities are in that case modifying an underlying already existing fingering pattern. If, on the contrary, the viscosity of  $A$  is equal to or larger than that of  $B$ , the nonreactive system is stable and any fingering pattern that arises in the reactive case can only be due to the chemical reactions. Podgorski *et al.* have first experimentally demonstrated this type of fingering fully triggered by reaction.<sup>11</sup> In their experiments, the solutions of  $A$  and  $B$  have the same viscosity while an  $A+B\rightarrow C$  chemical reaction produces a more viscous product  $C$ . The fingering dynamics is different whether  $A$  is in-

jected into  $B$  or vice versa, an asymmetry that can be induced by differences in diffusion coefficient or initial concentration of the two reactants for instance as shown numerically by Gérard and De Wit.<sup>12</sup>

From the theoretical point of view, nonlinear simulations of viscosity changes across miscible bistable autocatalytic chemical fronts have demonstrated chemically driven formation of droplets for instance.<sup>13–17</sup> For simple  $A+B \rightarrow C$  reactions, a modeling of the general case where the viscosity of the solution is a function of all species concentrations has been done by Hejazi *et al.* who have set up a reaction-diffusion-convection model to analyze the linear stability properties of reactive miscible fingering.<sup>18</sup> They show that the stability properties of such reactive systems depend typically whether the nonreactive case is already viscously unstable or not and whether the viscosity profile that builds up in time is monotonic in space or not. The stability properties were also demonstrated to crucially depend on time as the base state is itself time dependent. This approach has classified the various instability scenarios and has shown that chemical reactions can even destabilize the otherwise stable case of a more viscous solution pushing a less viscous one. Numerical simulations by Gérard and De Wit<sup>12</sup> have analyzed VF triggered by  $A+B \rightarrow C$  reactions when  $A$  and  $B$  have the same viscosity while  $C$  is more viscous as in the case of Podgorski *et al.*'s experiments.<sup>11</sup> More recently, Hejazi and Azaiez have extended this numerical study to some cases where the nonreactive limit is already unstable i.e., the displaced solution is more viscous than the invaded one.<sup>19</sup>

In this context, the objective of the present study is to complement these numerical studies of nonlinear miscible viscous fingering influenced or fully triggered by an  $A+B \rightarrow C$  chemical reaction by exploring systematically all possible cases, i.e., all situations whether the solution of  $A$  is less or more viscous than that of  $B$ . To do so, we numerically integrate the reaction-diffusion-convection model developed by Hejazi *et al.* coupling Darcy's law with a concentration dependent viscosity to equations for the evolution of the concentrations of the three chemicals  $A$ ,  $B$ , and  $C$ .<sup>18</sup> Our goal is to analyze the nonlinear fingering dynamics for various values of the relevant parameters to provide understanding of the later time evolution of the system. Our results shall be compared to those of linear stability analysis (LSA)<sup>18</sup> and experiments<sup>9,10</sup> of the same problem.

We will here focus on the infinite  $D_a$  case for which the numerical code can be simplified. Moreover, to allow comparison with the LSA of Hejazi *et al.*,<sup>18</sup> we will assume, along their approach, that all chemical species have the same diffusion coefficients and that both reactants  $A$  and  $B$  are initially present with the same concentration. The two important parameters of the problem are therefore the log-mobility ratios  $R_b$  and  $R_c$  quantifying the ratio of viscosities of the reactants  $B$  and  $C$  versus that of the reactant  $A$ , respectively.

Eventually, let us note that, in all experiments dealing with viscous fingering involving the influence of an  $A+B \rightarrow C$  type of chemical reaction,<sup>7,9–11</sup> the evolution of the fingering pattern is given by following the spatiotemporal distribution of a dye passive to the reaction and initially added in the displacing or the displaced fluid. Based on this

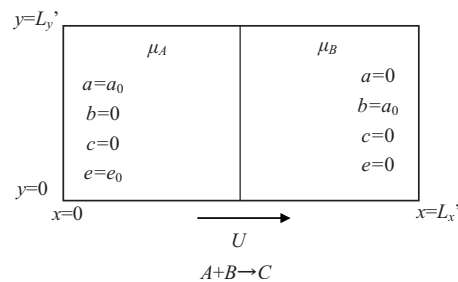


FIG. 1. Sketch of the system.

and to obtain nonlinear results to be compared to experiments, we also model the evolution of a passive dye as a fourth chemical species independent of the reaction. As will be shown later, this strategy is useful for quantitative characterization of the fingering pattern.

In this framework, the article is organized as follows. In Sec. II, the nonlinear equations of the model and the numerical scheme adapted to the infinite  $D_a$  condition are presented. In Sec. III, one-dimensional underlying reaction-diffusion viscosity profiles are classified in the  $(R_b, R_c)$  parameter plane. Results of the nonlinear simulations and of a parametric study are shown in Sec. IV. In Sec. V, a discussion including comparison with the LSA and experiments is made. Finally, we conclude the present study in Sec. VI.

## II. THE MODEL SYSTEM

### A. Basic equations

We consider a homogeneous two-dimensional porous medium of length  $L'_x$  and width  $L'_y$  with constant permeability  $\kappa$  as depicted in Fig. 1. Alternatively, this system also describes dynamics in a Hele–Shaw cell (two glass plates separated by a thin gap width  $l$ ) when  $l \ll L'_x, L'_y$  in which case  $\kappa = l^2/12$ . A solution of reactant  $A$  with viscosity  $\mu_A$  is injected from the left boundary with speed  $U$  along the  $x$  direction into a solution of reactant  $B$  with viscosity  $\mu_B$ . Both reactants  $A$  and  $B$  are initially present in the same initial concentration  $a_0$ . A chemical reaction  $A+B \rightarrow C$  takes place as soon as  $A$  and  $B$  are put in contact to yield the product  $C$ . In the present study, to follow the fingering pattern visually as done in experiments, we consider that a dye (species  $E$ ) is initially added in concentration  $e_0$  to the displacing solution. This dye is neutral to the chemical reaction and does not affect the viscosity of the solvent. As the system is considered incompressible and neutrally buoyant, the flow system is modeled using the continuity Eq. (1), Darcy's law Eq. (2) for the two-dimensional flow velocity  $\underline{u}=(u,v)$ , reaction-diffusion-convection Eqs. (3)–(5) for concentrations  $a$ ,  $b$ , and  $c$  of the chemical species  $A$ ,  $B$ , and  $C$ , and a diffusion-convection Eq. (6) for the concentration  $e$  of the dye  $E$ , namely,

$$\nabla \cdot \underline{u} = 0, \quad (1)$$

$$\nabla p = -\frac{\mu}{\kappa} \underline{u}, \quad (2)$$

$$\frac{\partial a}{\partial t} + \underline{u} \cdot \nabla a = D_A \nabla^2 a - kab, \quad (3)$$

$$\frac{\partial b}{\partial t} + \underline{u} \cdot \nabla b = D_B \nabla^2 b - kab, \quad (4)$$

$$\frac{\partial c}{\partial t} + \underline{u} \cdot \nabla c = D_C \nabla^2 c + kab, \quad (5)$$

$$\frac{\partial e}{\partial t} + \underline{u} \cdot \nabla e = D_E \nabla^2 e, \quad (6)$$

with appropriate boundary and initial concentrations. Here,  $p$  is the pressure,  $D_{A,B,C,E}$  are the diffusion coefficients of species  $A$ ,  $B$ ,  $C$ , and  $E$ , respectively, that are supposed to be equal here i.e.,  $D_A = D_B = D_C = D_E = D$ .  $k$  is the kinetic constant of the chemical reaction. In general,  $\mu = \mu(a, b, c)$ . We define  $\mu_A = \mu(a_0, 0, 0)$ ,  $\mu_B = \mu(0, a_0, 0)$ , and  $\mu_C = \mu(0, 0, a_0)$  as the viscosity of the solution when only one species  $A$ ,  $B$ , or  $C$ , respectively, is present in concentration  $a_0$ . Without loss of generality, the viscosity is scaled with the reference viscosity  $\mu_A$  of the  $A$  solution so that it depends eventually on the concentrations of  $B$  and  $C$  only. Following earlier studies,<sup>12-14,18,20</sup> the viscosity is chosen to vary exponentially on concentrations as

$$\mu = \mu_A \exp\left(R_b \frac{b}{a_0} + R_c \frac{c}{a_0}\right), \quad (7)$$

where the log-mobility ratios  $R_b$  and  $R_c$  are defined as

$$R_b = \ln\left(\frac{\mu_B}{\mu_A}\right) \quad \text{and} \quad R_c = \ln\left(\frac{\mu_C}{\mu_A}\right). \quad (8)$$

In absence of any reaction or if the product  $C$  has the same viscosity as one of the reactant ( $R_b = R_c$ ), the system is genuinely unstable if  $\mu_A < \mu_B$  ( $R_b > 0$ ). If  $R_b < 0$ , the nonreactive system is stable as we have then a displacement of a less viscous solution by a more viscous one.

We nondimensionalize the equations using the characteristic velocity  $U$ , hydrodynamical time  $\tau_h = D/U^2$  and length  $L_h = D/U$ . Concentration of species  $A$ ,  $B$ , and  $C$  are scaled by  $a_0$  and the concentration of the dye  $E$  by  $e_0$ . Viscosity is normalized by  $\mu_A$  and pressure by  $\mu_A D/\kappa$ . We further introduce the dimensionless Damköhler number

$$D_a = \frac{Dka_0}{U^2}, \quad (9)$$

which corresponds to the ratio between the hydrodynamic time  $\tau_h$  and the chemical reaction time  $\tau_c = 1/ka_0$ . Switching to a reference frame moving with the injection speed  $U$ , taking the curl of Darcy's law and introducing the stream function  $\psi(x, y)$  defined such that  $u = \partial\psi/\partial y$  and  $v = -\partial\psi/\partial x$ , we have<sup>20</sup>

$$\nabla^2 \psi = -R_b(\psi_x b_x + \psi_y b_y + b_y) - R_c(\psi_x c_x + \psi_y c_y + c_y), \quad (10)$$

$$a_t + a_x \psi_y - a_y \psi_x = \nabla^2 a - D_a ab, \quad (11)$$

$$b_t + b_x \psi_y - b_y \psi_x = \nabla^2 b - D_a ab, \quad (12)$$

$$c_t + c_x \psi_y - c_y \psi_x = \nabla^2 c + D_a ab, \quad (13)$$

$$e_t + e_x \psi_y - e_y \psi_x = \nabla^2 e, \quad (14)$$

$$\mu = \exp(R_b b + R_c c). \quad (15)$$

## B. Infinite $D_a$ case

From here on, we consider Eqs. (10)–(15) under the condition of infinite  $D_a$  i.e., infinitely fast chemical reactions. Subtracting Eq. (12) from Eq. (11) and adding Eq. (11) to Eq. (13) we get, respectively,

$$(a - b)_t + (a - b)_x \psi_y - (a - b)_y \psi_x = \nabla^2(a - b), \quad (16)$$

$$(a + c)_t + (a + c)_x \psi_y - (a + c)_y \psi_x = \nabla^2(a + c), \quad (17)$$

We then introduce two conserved scalars  $Z_1$  and  $Z_2$ , which are independent of the chemical reaction, as follows:

$$Z_1 = a - b, \quad (18)$$

$$Z_2 = a + c. \quad (19)$$

These conserved scalars can be normalized in the form

$$z_i = \frac{Z_i - Z_{i,B0}}{Z_{i,A0} - Z_{i,B0}}, \quad (20)$$

where  $i=1, 2$  while  $Z_{i,A0}$  and  $Z_{i,B0}$  are the values of  $Z_i$  in the pure displacing and displaced fluid, respectively. Therefore in the displacing fluid,  $z_i=1$ , while in the displaced fluid,  $z_i=0$ . Regarding  $Z_1 = a - b$ , because  $Z_{1,A0} = 1$  and  $Z_{1,B0} = -1$ , we obtain

$$z_1 = \frac{(a - b) + 1}{2}. \quad (21)$$

Regarding  $Z_2 = a + c$ , because  $Z_{2,A0} = 1$ ,  $Z_{2,B0} = 0$ , we obtain

$$z_2 = a + c. \quad (22)$$

It should be noted that now  $Z_1$  and  $Z_2$  are normalized between 0 and 1 and thus  $z_1 = z_2 = z$ . The idea is then to integrate the equation for  $z$  and reconstruct the concentrations fields  $a$ ,  $b$ , and  $c$  from it. This idea is commonly used in combustion science and was also used to study turbulent reacting liquid flows.<sup>21</sup>

Under the condition of infinite  $D_a$ , the chemical reaction takes place in an infinitesimally thin region called here the reaction front. At the reaction front, the concentration of the reactants  $a$  and  $b$  tend to 0, while  $z$  becomes  $z_{st}$  (subscript st stands for stoichiometry) which takes the value  $z_{st} = 0.5$  from Eq. (21). When  $z < z_{st}$ ,  $a = 0$ ,  $b = 1 - 2z$  from Eq. (21) and  $c = z$  from Eq. (22). When  $z > z_{st}$ ,  $b = 0$ . Thus we obtain  $a = -1 + 2z$  from Eq. (21) and  $c = 1 - z$  from Eq. (22).

In summary, under the condition of infinite  $D_a$ , analyzing the system of Eqs. (10)–(14) can be reduced to solving the equations

$$\nabla^2 \psi = -R_b(\psi_x b_x + \psi_y b_y + b_y) - R_c(\psi_x c_x + \psi_y c_y + c_y), \quad (23)$$

$$z_t + z_x \psi_y - z_y \psi_x = \nabla^2 z, \quad (24)$$

along with the condition that, for  $z < z_{st}$ , we have

$$(a, b, c) = (0, 1 - 2z, z) \quad (25)$$

while if  $z > z_{st}$ ,

$$(a, b, c) = (-1 + 2z, 0, 1 - z). \quad (26)$$

It should be noted that the dye concentration  $e$  follows exactly the same dynamics as  $z$ . In these dimensionless scales, the dimensionless domain width and length are denoted as  $L_x = UL'_x/D$  and  $L_y = UL'_y/D$ . In these conventions,  $L_y$  determines the number of fingers present across the domain, and  $L_x$  dictates the maximum time of the simulations.

### C. Numerical method

To numerically solve Eqs. (23)–(26), we have adapted the pseudospectral numerical scheme described in Tan and Homsy to take into account the infinite  $D_a$  condition.<sup>22</sup> The boundary conditions are taken periodic in both directions. As has been shown in many previous studies (see Gérard and De Wit<sup>12</sup>), the use of such boundary conditions has no influence on the dynamics of the chemical front as long as the unstable propagating front does not encounter its periodic extension. As initial conditions, we consider a constant linear velocity  $U$  corresponding to a zero velocity relative to the moving frame, i.e.,  $\psi=0$  everywhere. For the concentrations, we take a step front between the reactive solutions of  $A$  and  $B$  with  $c=0$  everywhere and random noise added in the front to trigger the instability on reasonable computing time. To validate the code, we have checked that the nonlinear simulations reproduce the predicted wavelength given by the LSA<sup>18</sup> and that the evolution of the fingering pattern is robust with time and spatial steps refinement.

### III. BASE STATE REACTION-DIFFUSION VISCOSITY PROFILES

Viscous fingering instabilities are triggered when a less viscous fluid displaces another more viscous one either globally or at least locally somewhere in the system when viscosity profiles vary nonmonotonically in space. Previous works have shown in nonreactive systems that the nonmonotonic character of the viscosity profile can play an important role on the fingering dynamics.<sup>23–26</sup>

To analyze here the role of each parameter of the problem and of possible chemically driven nonmonotonic viscosity profiles on the related nonlinear fingering dynamics, base state viscosity profiles are therefore constructed for given values of  $R_b$  and  $R_c$  on the basis of the underlying one-dimensional  $A+B \rightarrow C$  reaction-diffusion system. Following the reasoning of Rongy *et al.*<sup>27</sup> for density profiles, Hejazi *et al.*<sup>18</sup> found that the viscosity profile is monotonically increasing when  $0 \leq R_c \leq 2R_b$ , while it is monotonically decreasing when  $2R_b \leq R_c \leq 0$ . In contrast, the viscosity profile is nonmonotonic and features an extremum when  $R_c[R_b - (R_c/2)] \leq 0$ . In Fig. 2, a sketch of the six different possible viscosity profiles are illustrated in the  $(R_b, R_c)$  plane.<sup>18</sup> The condition  $R_c = R_b$  means that the viscosity of the product  $C$  is equal to

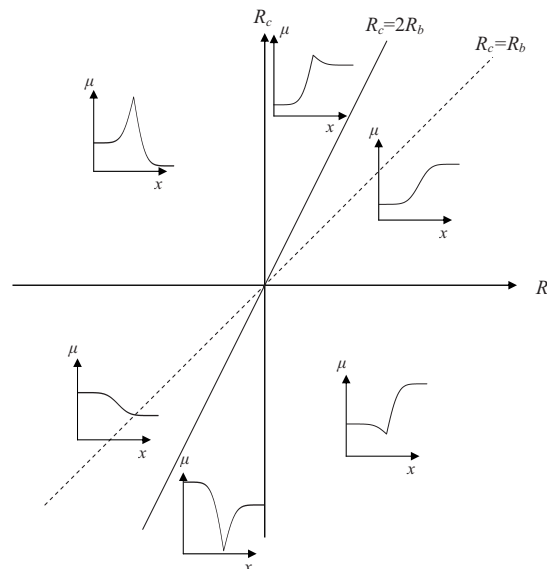


FIG. 2. Viscosity profiles in the  $(R_b, R_c)$  plane. The lines  $R_c = 2R_b$  and  $R_c = 0$  delimit the zone of monotonic viscosity profiles. The line  $R_c = R_b$  corresponds to the peculiar case where the viscosity profile is exactly the same as in absence of reaction.

that of the displaced reactant  $B$ . In this case, the viscosity profile is antisymmetric with respect to  $x = L_x/2$  and is the same as that without reaction. In the present paper, we will discuss the effect of changes in  $R_c$  for various values of  $R_b$ .

### IV. NONLINEAR FINGERING DYNAMICS IN REACTIVE SYSTEMS

Numerical simulations are performed for different values of the log-mobility ratios  $R_b$  and  $R_c$ . Before proceeding to a parametric study, let us first analyze typical concentration patterns in both reactive and nonreactive cases.

#### A. Concentration fields

As mentioned in the introduction, in most cases, the fingering pattern is followed in experiments by imaging the distribution of a dye initially added to the displacing fluid. We will therefore analyze here the fingering pattern not only by inspecting the concentrations of  $A$ ,  $B$ , and  $C$  but also the concentration of a passive scalar  $E$  added initially to the reactant  $A$ . To follow the nonlinear VF dynamics, we typically plot 2D concentration fields on a gray scale ranging from 0 in white to 1 in black for  $A$ ,  $B$ , and  $E$  or 0.5 in black for  $C$ .

Let us start by showing in Fig. 3 a typical reactive VF pattern for an infinite Damköhler number  $D_a$  in the peculiar case where  $R_c = R_b$ , i.e., when the underlying viscosity profile is equivalent to that of the nonreactive case. The concentration fields of the reactants  $A$  and  $B$  are different than those observed in the nonreactive case as they are consumed in the reaction zone. As the product  $C$  is generated at the interface with a viscosity equal to that of  $B$  as  $R_c = R_b$ , the dye is however advected by exactly the same fingering dynamics than in the nonreactive case.

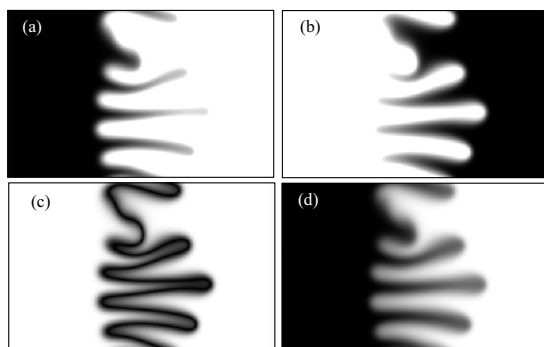


FIG. 3. Concentration of (a) reactant  $A$ , (b) reactant  $B$ , (c) product  $C$ , and (d) dye  $E$  in reactive fingering for  $R_c = R_b = 2$  at  $t = 1000$  with  $L_x = 1024$ .

As soon as  $R_c \neq R_b$ , this will not be the case anymore as shown in Fig. 4. The product  $C$  has here a lower viscosity than the reactant  $B$  and the fingering pattern for the dye and all other chemicals is different from the one of the nonreactive case. Note that the evolution of  $A$  and  $E$  are here significantly different even though these two species were both initially present in the displacing solution and have the same diffusion coefficient. This difference is directly correlated with the reaction which has here consumed the reactant  $A$  around the fingertips. We also note that the wavelength of the pattern for  $R_c = 0$  (Fig. 4) is smaller than for  $R_c = 2$  (Fig. 3) which is in agreement with the LSA of Hejazi *et al.*<sup>18</sup> showing that decreasing  $R_c$  below  $R_b$  when  $R_b > 0$  has a destabilizing effect. Let us now analyze the changes in fingering patterns when the log-mobility ratios are varied. The parameter plane can essentially be divided in two zones depending whether the displacing solution of  $B$  is more ( $R_b > 0$ ) or less ( $R_b < 0$ ) viscous than the injected solution of  $A$ . Let us focus on these two situations successively.

### B. Reactive fingering when $R_b > 0$

If  $R_b > 0$ , then the nonreactive equivalent case is viscously unstable and we analyze to what extent the chemical reaction will modify the fingering pattern. To do so, let us present numerical results obtained at a fixed  $R_b = 2$  for various values of  $R_c$  in the range of  $-2 \leq R_c \leq 6$ . Corresponding base state reaction-diffusion concentration and viscosity profiles are shown in Fig. 5 as a function of  $(x - L_x/2)$  for both reactive and nonreactive cases. In absence of reaction, the

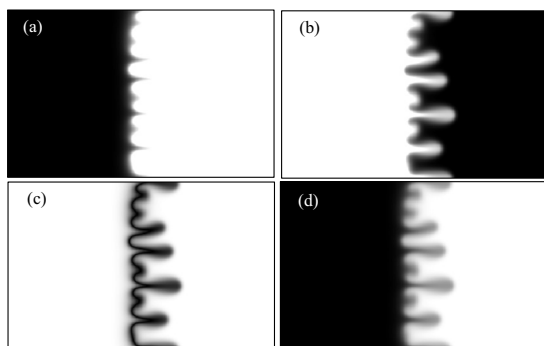


FIG. 4. Same as Fig. 3 for  $R_c = 0$ ,  $R_b = 2$  at  $t = 500$ .

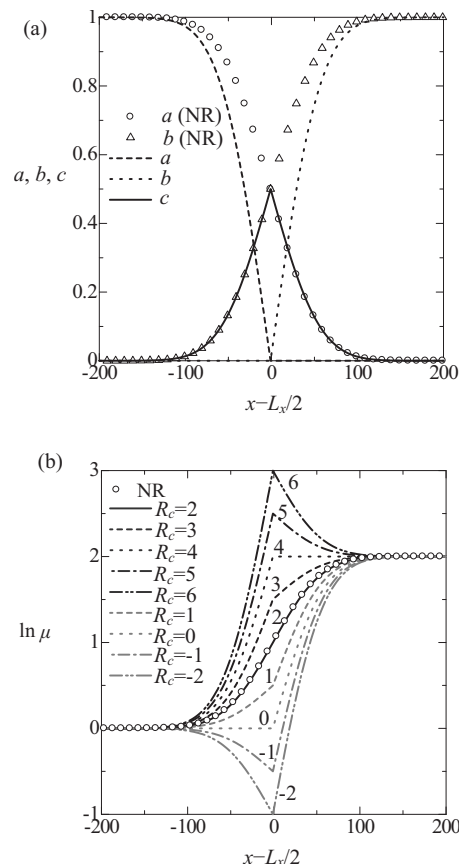


FIG. 5. Long time asymptotic 1D reaction-diffusion (a) concentration and (b) viscosity profiles for various  $R_c$  at  $R_b = 2$ . The notation “NR” stands for “nonreactive.”

concentration profiles of the passive scalars  $A$  and  $B$  evolve following an error function which gives (as  $R_b > 0$ ) an unstable viscosity profile increasing monotonically along  $x$ . In the special case where  $R_c = R_b$ , the consumption of  $B$  by the reaction is exactly balanced in the viscosity profile by the production of  $C$  which has the same viscosity than  $B$ . Fingering is then exactly the same as in the nonreactive case. If  $R_c > R_b$ , the product  $C$  is more viscous than  $B$  and the viscosity is increased in the reaction zone. The viscosity profile becomes nonmonotonic with a maximum once  $R_c > 2R_b$ . Analogous situations are obtained for  $R_c < R_b$  with nonmonotonic profiles with a minimum developing if  $R_c < 0$ . Note on Fig. 5(b) that the two conditions corresponding to a fixed  $|R_b - R_c|$  yield symmetric viscosity profiles with respect to the nonreactive case  $R_c = R_b$ .

Figure 6 shows the temporal evolution of fingering patterns of the dye for the various viscosity profiles displayed in Fig. 5 for  $R_c \geq R_b$ . When  $R_c = R_b$  ( $= 2$  here), fingering dynamics is exactly the same as in the nonreactive fingering case. This case is moreover the most stable situation where fingering appears as last. The larger the difference  $|R_b - R_c|$ , the quicker the onset of fingering. This confirms predictions of the LSA<sup>18</sup> that the reactive situations are always more unstable than their nonreactive counterpart for relatively large time. For what concerns the nonlinear dynamics, we observe no major difference whether the viscosity profile is nonmonotonic or not. Indeed, the evolution of the fingers is

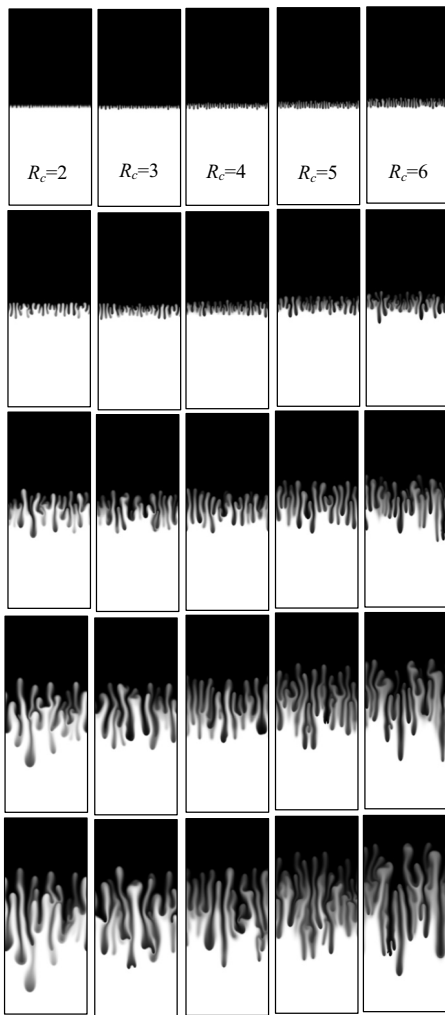


FIG. 6. Fingering dynamics for various  $R_c \geq R_b=2$  shown at time  $t=400, 800, 1600, 2400,$  and  $3200$  from top to bottom in a system of width  $L_y=2048$ .

smoothly changing when  $R_c$  is varied. The noticeable trends are however that fingers get thinner and more numerous when  $R_c$  is increased above  $R_b$ . Their center of mass is also displaced toward the back as they extend more in the reverse than in the forward direction when  $R_c$  increases.

If, on the contrary,  $R_c$  is decreased below  $R_b$  at fixed  $R_b=2$  i.e., if the product  $C$  is less viscous than the reactant  $B$  (Fig. 7), the instability also appears earlier than in the non-reactive case. However, coarsening and shielding are more efficient and the number of fingers is decreasing while tip splitting events are more often encountered. Moreover, in that case, fingers develop more along the flow and forward fingering is observed to be more active.

### 1. Quantitative measurements

To corroborate these qualitative observations by quantitative data, let us introduce several quantitative evaluations.<sup>12</sup> First of all, the two-dimensional concentration field of the dye,  $e(x,y,t)$ , can be averaged along the transverse coordinate  $y$  to yield one-dimensional (1D) transversely averaged concentration profiles

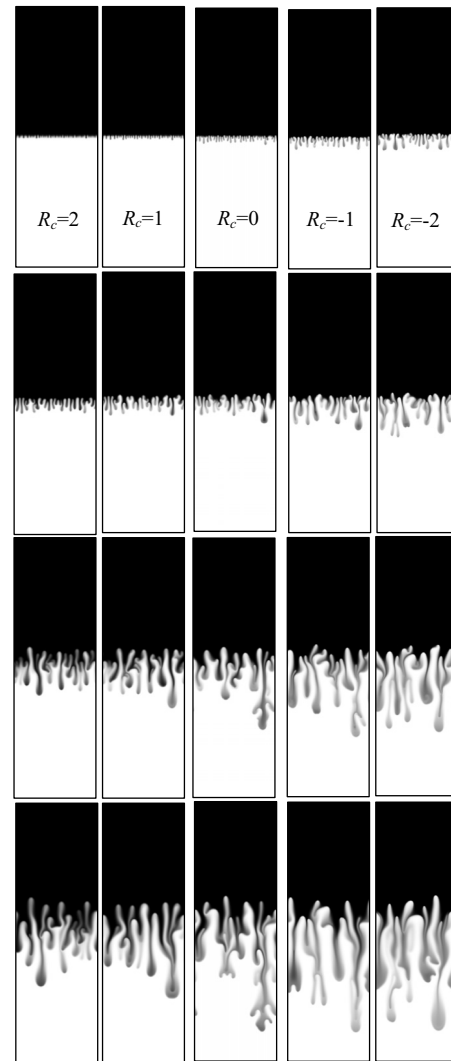


FIG. 7. Same as Fig. 6 but for various  $R_c \leq R_b=2$  shown at time  $t=400, 800, 1600,$  and  $2400$  from top to bottom.

$$\langle e(x,t) \rangle = \frac{1}{L_y} \int_0^{L_y} e(x,y,t) dy. \quad (27)$$

An example of such a profile  $\langle e(x,t) \rangle$  is drawn in Fig. 8. On the basis of this 1D profile, we next define a reverse mixing length  $L_-$  (Ref. 24) as the distance between the position  $L_-$

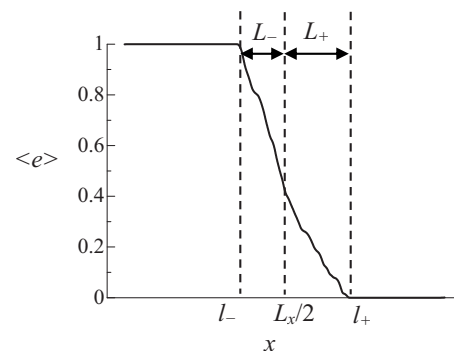


FIG. 8. Illustration of the mixing lengths  $L_-$  and  $L_+$  on the transversely averaged concentration profile  $\langle e \rangle$  of the dye.

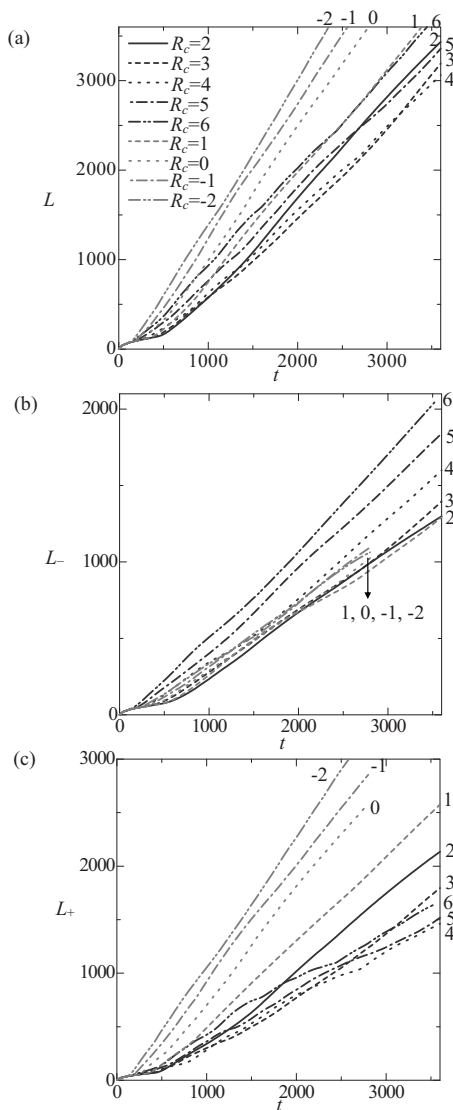


FIG. 9. Temporal evolution of (a) the total  $L$ , (b) reverse  $L_-$ , and (c) forward  $L_+$  mixing lengths for various  $R_c$  at fixed  $R_b=2$ . Each curve is obtained by averaging the results of five simulations.

along  $x$  where  $\langle e(x,t) \rangle$  becomes lower than 0.99 and the position  $x=L_x/2$  of the initial interface. A forward mixing length  $L_+$  is similarly defined as the distance between  $x=L_x/2$  and the position  $l_+$  where  $\langle e(x,t) \rangle$  becomes lower than 0.01 (Fig. 8). The total mixing length  $L$  is next defined as

$$L = L_- + L_+. \quad (28)$$

Figure 9 shows the growth of  $L$ ,  $L_-$ , and  $L_+$  in time for the parameter values of Figs. 6 and 7, i.e., for a fixed  $R_b=2$  and  $R_c$  in the range  $[-2, +6]$ . Each curve is the average of five runs made with the same values of  $R_b$  and  $R_c$  but different initial distribution of the noise. In all cases, at early time,  $L$ ,  $L_-$ , or  $L_+$  increase as  $t^{1/2}$ , which characterizes the initial mixing by diffusion until they jump up when fingering starts to occur. Fingering occurs the latest when  $R_c=R_b$ , the equivalent of the nonreactive case. This confirms that the reaction always increases the destabilization of the system. Moreover, the larger  $|R_b-R_c|$ , the earlier the onset of VF instability.

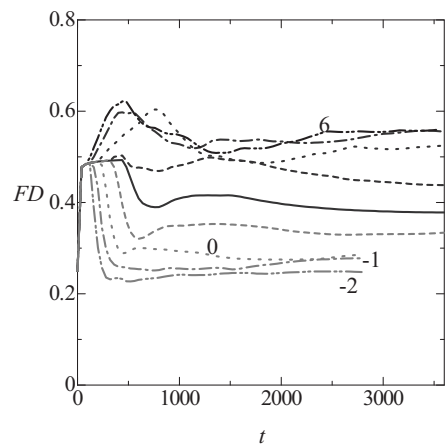


FIG. 10. Temporal evolution of the finger density  $FD$  for various  $R_c$  at fixed  $R_b=2$ . Each curve is obtained by averaging the results of five simulations.

Comparing symmetric conditions (i.e., fixed  $|R_b-R_c|$ ), the time at which fingering starts is almost the same. The corresponding LSA for large  $D_a$  (Ref. 18) has shown that the stability was different depending whether  $R_c > R_b$  or  $R_c < R_b$  for early times ( $t < 5$ ) including  $t=0$ . For larger times ( $t > 5$ ) however, the LSA shows that the reaction always destabilizes the system if  $R_c \neq R_b$  and the extent of this destabilization is the same for symmetric conditions ( $|R_b-R_c|$ ). Comparison between the present nonlinear simulations and the LSA points to the fact that the results of the LSA for large times dominantly characterize the nonlinear simulation results where fingering starts at  $t > 100$ .

Next, let us focus on the evolution of the mixing lengths for later time (Fig. 9). When  $R_c \geq R_b$ ,  $L_-$  increases with  $|R_b-R_c|$ , while  $L_+$  is smaller. Except for  $R_c=6$ ,  $L$  is smaller than in the nonreactive case. When  $R_c \leq R_b$ , in contrast,  $L_+$  increases with  $|R_b-R_c|$ , while  $L_-$  is similar and hence  $L$  increases. We can compare  $L$  with the length of the longest finger in the corresponding experiment.<sup>9</sup> In the experiment, the length of the longest finger at a later given time in the reactive case was smaller for  $R_c > R_b$  whereas larger for  $R_c < R_b$  than that in the nonreactive case. Therefore, the present simulation results for  $L$  have a good agreement with the experimental results.

Another useful quantitative measure is the fingering density  $FD$  defined as

$$FD(t) = \frac{1}{L_y \times L} \int_0^{L_y} \int_{l_-}^{l_+} e(x,y,t) dx dy. \quad (29)$$

This quantity corresponds to the amount of dye present in the mixing zone. If the fingering pattern becomes denser,  $FD$  becomes larger and vice versa. In addition, this parameter can be used for direct comparison with the corresponding experimental results for radial fingering<sup>9</sup> where  $FD$  has been defined as the area occupied by the pattern in a circle the radius of which is the length of the longest finger. As shown in Fig. 10, when  $R_c \leq R_b$ ,  $FD$  decreases as  $|R_b-R_c|$  increases, while it becomes larger for  $R_c \geq R_b$ . The results for the cases involving monotonic viscosity profiles ( $R_c=0-4$ ), as is the case in the experiments, have good agreement with the cor-

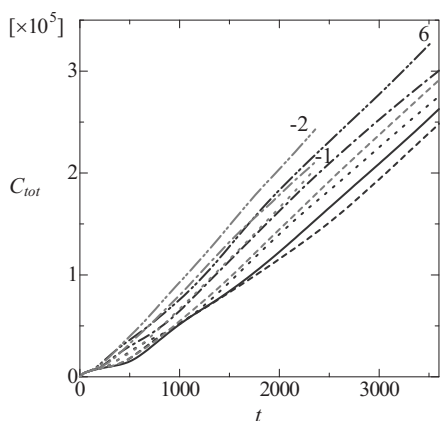


FIG. 11. Total amount of product  $C_{\text{tot}}$  produced in time for various  $R_c$  at fixed  $R_b=2$  in the domain defined by  $L_x < x < 7L_x/8$  and  $0 < y < L_y$  with  $L_x=8192$ ,  $L_y=2048$ . Each curve is the average of five simulations.

responding experimental results in which the fingering density becomes larger (smaller) when a more (less) viscous product is produced.

Eventually, from a chemical engineering point of view, it is interesting to compute  $C_{\text{tot}}$ , the total amount of product  $C$  generated at a given time, to see whether the fingering instability can increase the production rate of the reaction or not. We measure  $C_{\text{tot}}$  as the integral of  $c$  in the region  $L_x/8 < x < 7L_x/8$  over the whole  $L_y$ . Figure 11 shows the temporal evolution of  $C_{\text{tot}}$  for the simulations of Figs. 6 and 7. We find that  $C_{\text{tot}}$  at an arbitrary fixed  $t$  is generally larger for  $R_c \neq R_b$  than for  $R_c = R_b$ . Moreover, except for  $R_c=3$ ,  $C_{\text{tot}}$  becomes larger as the underlying viscosity profile is further departing from that of the nonreactive case i.e., when  $|R_b - R_c|$  increases.

On the basis of these quantitative measures, let us now analyze into more details the specific influence of  $R_c$  at a fixed value of  $R_b$ .

## 2. Influence of $R_c$

*a.  $2R_b \geq R_c > R_b$ .* In this case, the product  $C$  is more viscous than the reactant  $B$  but the underlying viscosity profile is still increasing monotonically along  $x$  [see Fig. 5(b)]. Fingering starts earlier and, as seen on Fig. 6 and quantitatively confirmed in Fig. 10, the pattern also becomes denser. Concerning the longitudinal extent of the fingers (Fig. 9), the total mixing length  $L$  is larger than in the nonreactive case just after VF onset because the gradient of the viscosity profile is sharpening in the trailing zone [i.e., zone located at  $(x - L_x/2) < 0$ , see Fig. 5(b)] when  $R_c$  increases above  $R_b$ . However, later on, this trend is reversed as, for longer times, the total mixing length  $L$  (and particularly  $L_+$ ) for  $R_c=3$  and 4 starts to slow down and ultimately becomes smaller than the value for  $R_c=R_b$ .

To understand why this is the case, let us have a close inspection to Fig. 12 which provides a focus at a given later time in the spatiotemporal distribution of the concentration, viscosity and velocity fields. Here velocity means the magnitude of velocity being equal to  $\sqrt{u^2 + v^2}$ . In the reference case  $R_c=2$  presented in Fig. 12(a), the largest velocity is on average always located in the most advanced finger and sets the speed of growth of the mixing length. If  $R_c=4$  as displayed on Fig. 12(b), the most advanced finger in the dye representation corresponds to a highly reactive zone producing a large amount of more viscous product  $C$  and where the flow is thus slowed down. Larger velocity regions develop therefore in adjacent fingers. An alternation of acceleration of neighboring fingers followed by their speed down when

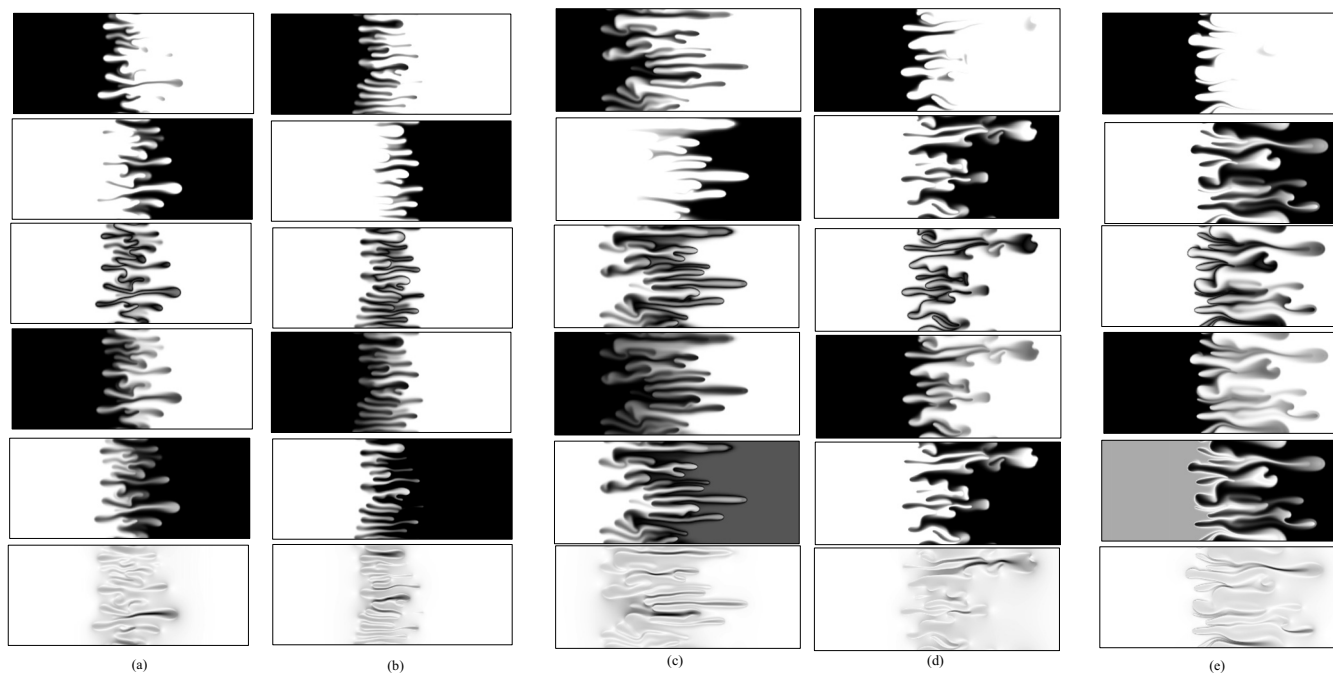


FIG. 12. Concentration of  $A$ ,  $B$ ,  $C$ , and dye  $E$ , viscosity and velocity fields shown from top to bottom for  $R_b=2$  and (a)  $R_c=2$  at time  $t=2000$ , (b)  $R_c=4$  at time  $t=2000$ , (c)  $R_c=6$  at time  $t=2800$ , (d)  $R_c=0$  at time  $t=2000$ , and (e)  $R_c=-2$  at time  $t=2000$ .

they become the leading fingers is observed which leads to a decrease in the forward growth of fingers (and hence in  $L_+$  and  $L$ ). In addition, the alternation of acceleration of neighboring fingers leads to a competition in growth of the fingers and results in an increase of the fingering density.

*b.  $R_c > 2R_b$ .* If  $R_c > 2R_b$ , the product is viscous enough to yield a nonmonotonic viscosity profile with a maximum. In this case, the reaction is further destabilizing the system as the overall viscosity jump is increasing between the reference viscosity of  $A$  and that of the increasing maximum [Fig. 5(b)]. The unfavorable viscosity jump is located on the trailing zone of the nonmonotonic viscosity profile favoring reverse fingering ( $L_- \gg L_+$ ). This is all the more true as the fingers that develop on the trailing zone encounter a stable barrier in the leading zone [i.e., zone where  $(x - L_x/2) > 0$ ] that prevents them from further growth in the flow direction.<sup>28</sup> Focusing on  $L$  for later times [Fig. 9(a)], both situations in which  $L$  is larger or smaller than in the nonreactive case occur because of the competition, when  $R_c$  increases, between the increasing viscosity jump which enhances fingering and the increasing stable barrier in the frontal zone which suppresses fingering. In Fig. 12(c), it is seen that the highest velocity is located in the adjacent finger.

*c.  $0 \leq R_c < R_b$ .* In this case, the viscosity of the product is smaller than that of the reactant  $B$  but yet the viscosity profile remains monotonic. Fingering still occurs earlier than in the nonreactive equivalent  $R_c = R_b$  as observed in Fig. 7. In the long time nonlinear regime, the total mixing length remains larger, forward fingering and tip splitting are especially more intense as the viscosity gradient is sharper in the leading zone [Fig. 5(b)]. Moreover, a close inspection of Fig. 12(d) for  $R_c = 0$  shows that in the most advanced finger in the dye representation, the concentration of the less viscous product  $C$  is large which favors flow into this most advanced finger and thus an efficient increase of  $L$ . This also enhances shielding of this most advanced finger on its neighbors leading to a decrease in the finger density FD (Fig. 10).

*d.  $R_c < 0$ .* Eventually, if  $R_c < 0$ , a nonmonotonic viscosity profile develops with a minimum [Fig. 5(b)] and an unstable leading zone where the less viscous product  $C$  displaces the more viscous reactant  $B$ . As the viscosity jump is increased when  $R_c$  is decreased below 0, the situation becomes more unstable with forward fingering being more and more dominant as seen on Fig. 9(c). Figure 12(e) shows that, in this case, the lower viscosity region is located in the middle of the fingers while the largest speed is located in the most advanced finger of the dye distribution. Interestingly, we note that the reactant  $A$  is totally consumed in the advancing fingers, an effect which increases when  $R_c$  decreases.

### 3. Remarks

It is here interesting to compare the two monotonic situations for  $R_c = 0$  and  $R_c = 4$  (same  $|R_b - R_c|$  but  $R_c < R_b$  or  $R_c > R_b$ , respectively) which have the same overall unfavorable viscosity jump between  $A$  and  $B$  as in the nonreactive case, yet they are both more unstable as the viscosity gradient is larger than for  $R_c = R_b$ , respectively, in the leading zone ( $R_c < R_b$ ) or trailing zone ( $R_c > R_b$ ) [Fig. 5(b)]. However, the

nonlinear dynamics is not symmetric:  $R_c = 0$  is much more unstable than the case  $R_c = 4$  which is coherent with predictions of the LSA.<sup>18</sup>

Asymmetries also exist when comparing the nonmonotonic situation with a minimum for  $R_c = -2$  with the one with a maximum for  $R_c = 6$  both having the same viscosity jump. The situation with a minimum ( $R_c < 0$ ) provides fewer fingers, enhancement of the shielding effect, decrease of the finger density FD and dominance of forward fingering in the leading zone where the unstable viscosity jump is located. The presence of a maximum in the viscosity profile ( $R_c > 2R_b$ ) on the contrary, features smaller thin fingers with an increase of FD and longer extension of the fingers in the reverse direction where the unfavorable viscosity ratio is present. Even for symmetric values of  $|R_b - R_c|$ , fingering is observed to be much more effective and yield larger total mixing lengths for  $R_c < 0$ . This is coherent with the fact that fingering has been shown in nonreactive systems to be more effective when fingers develop along the flow than against it.<sup>28</sup> We recover here the same effect: fingers develop more easily along the flow on the unstable forward zone when  $R_c < 0$ . In the presence of a maximum in viscosity ( $R_c > 2R_b$ ), they grow on the contrary on the back of the nonmonotonic profile and encounter a stable barrier ahead of them which hinders their growth.

To sum up the results described above for  $R_b > 0$ , we find that, for  $R_c \geq R_b$ , fingers become thinner and more stretched, the finger density increases while reverse fingering is favored. The total mixing length  $L$  is smaller on the long time than in the nonreactive equivalent for intermediate values of  $R_c \geq R_b$  due to the fact that the increase of viscosity by the reaction at the tip of the most advanced finger is slowing it down. Larger  $L$  is nevertheless obtained for even larger  $R_c$  when the increase in the viscosity jump due to the reaction takes over. For  $R_c \leq R_b$ , shielding is favored giving rise to larger and less numerous fingers extending preferably in the forward direction where the viscosity jump is displaced. The total mixing length is always larger than in the nonreactive case.

### C. Reactive fingering when $R_b < 0$

If  $R_b < 0$ , the displacing solution of reactant  $A$  is more viscous than the displaced solution of reactant  $B$  and the system is genuinely stable in absence of any reaction. Any fingering instability can then only be triggered by the chemical reaction. The case of reactants of equal viscosity ( $R_b = 0$ ) has already been examined experimentally by Podgorski *et al.*<sup>11</sup> and numerically by Gérard and De Wit<sup>12</sup> but this case is only a peculiar limit of the nonmonotonic viscosity profiles.

As seen on Figs. 2 and 13, the viscosity profile decreases monotonically from  $\mu_A$  to  $\mu_B$  provided  $2R_b \leq R_c \leq 0$  and the chemical reaction cannot destabilize the system in that case. If  $R_c > 0$ , a nonmonotonic viscosity profile with a maximum builds up with the unfavorable viscosity jump located on the trailing zone. Reverse fingering is expected to be favored in this situation. On the contrary, if  $R_c < 2R_b < 0$ , a minimum in

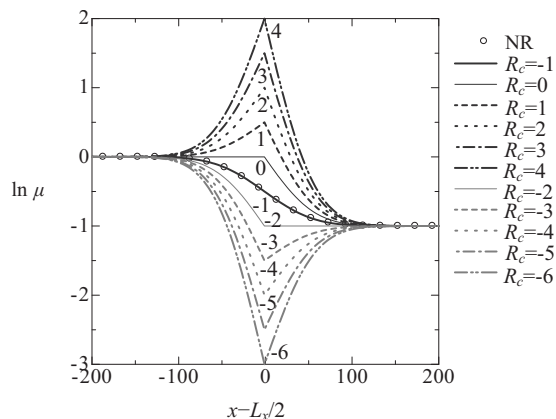


FIG. 13. Long time asymptotic 1D reaction-diffusion viscosity profiles for various  $R_c$  at  $R_b=-1$ . The notation NR stands for nonreactive.

viscosity appears and the unstable zone is shifted toward the leading zone where forward fingering is anticipated to develop.

These predictions are fully borne out by numerical simulations as seen on Fig. 14 for the special case  $R_b=-1$ . The larger the difference  $|R_b-R_c|$ , the more unstable the system with fingering starting earlier and fingers extending further away with hence a larger mixing length  $L$  for a same fixed time. The fingering density significantly varies as well with denser or less dense fingering observed for  $R_c > 0$  or  $R_c < 2R_b < 0$ , respectively (Fig. 16).

In Fig. 15 showing the temporal evolution of the mixing lengths, it is confirmed that for the initial stage, the larger  $|R_b-R_c|$ , the earlier the fingering occurs. In addition, for symmetric conditions, that is, at fixed  $|R_b-R_c|$  ( $R_c=+2$  versus  $-4$  or  $+3$  versus  $-5$  or also  $+4$  versus  $-6$ ), the time at which fingering starts is almost the same. The corresponding LSA for large  $D_a$  (Ref. 18) has shown that the stability is different depending whether  $R_c > 0$  or  $R_c < 2R_b < 0$  for early times but become equivalent at later times (when  $t > 100$ ).

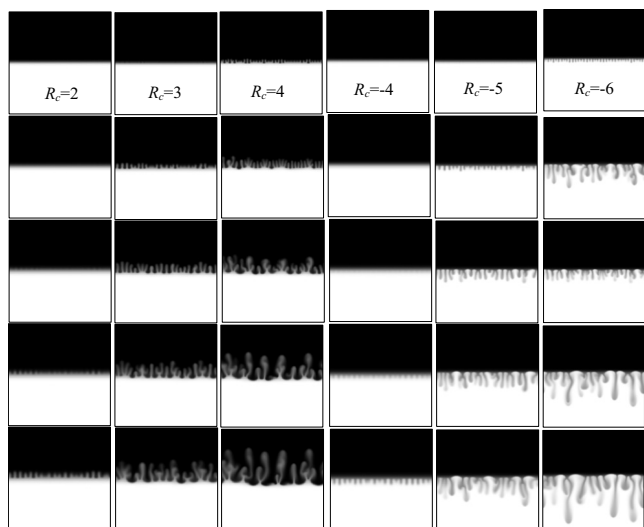


FIG. 14. Concentration of the dye  $E$  in reaction-induced fingering for various  $R_c$  at fixed  $R_b=-1$  shown at time  $t=400, 800, 1200, 1600$ , and  $2000$  from top to bottom in a system of width  $L_y=2048$ .

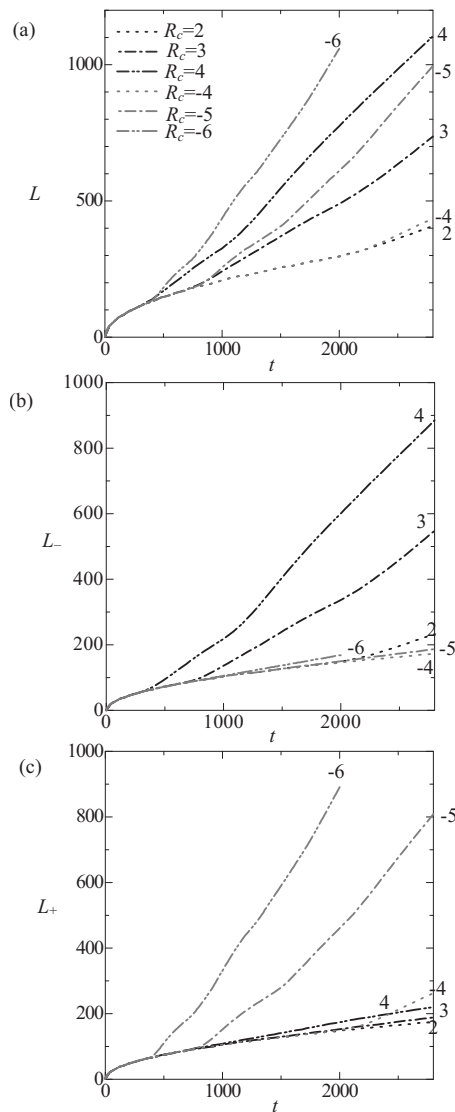


FIG. 15. Temporal evolution of (a) the total  $L$ , (b) reverse  $L_-$ , and (c) forward  $L_+$  mixing lengths for various  $R_c$  at fixed  $R_b=-1$ . Each curve is the average of three simulations.

Our simulations indicate that the results of the LSA for later times dominantly characterize the nonlinear dynamics where fingering starts at  $t > 400$ .

A close inspection to the temporal dependence of the mixing lengths (Fig. 15), the fingering density  $FD$  (Fig. 16) and the total amount of product  $C_{tot}$  (Fig. 17) shows that, once more the situation is not symmetric for a same viscosity jump depending whether a maximum or a minimum in viscosity is developing. This is again related to the easier growth of forward fingering along the flow in the leading zone when there is a minimum in the viscosity compared to the reverse situation with a maximum when fingers must develop against the flow on the trailing zone and encounter a stable barrier in the leading zone.

Finally, it is interesting to compare the dynamics of the various variables for symmetric  $|R_b-R_c|$  cases at a given later time at  $R_b=-1$  for, respectively,  $R_c=4$  (maximum) and  $-6$  (minimum) in Fig. 18. In the presence of a maximum, the fingering zone of the dye contains both reactant  $A$  and

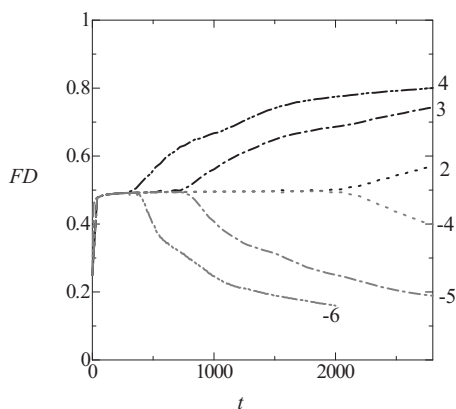


FIG. 16. Temporal evolution of the finger density  $FD$  for  $R_b = -1$  and various values of  $R_c$ . Each curve is the average of three simulations.

product  $C$  but no reactant  $B$ . A viscously stable barrier is seen in the viscosity distribution. Larger positive (negative) values of the velocity are located in the forward (reverse) fingers of the dye. In the presence of a minimum on the contrary, the fingering zone of the dye contains both reactant  $B$  and product  $C$  but no reactant  $A$ . In the viscosity distribution, the less viscous product is seen to displace the reactant  $B$ . The advanced fingers have on average larger velocities.

## V. COMPARISON WITH LSA AND EXPERIMENTS

In this section, we summarize and further discuss comparisons between the present numerical simulation results and the corresponding LSA and experimental results. The nonlinear simulations confirm the important role that chemical reactions have on fingering properties when the viscosity of the solution depends on the concentration of the chemical species involved. First of all, the trends predicted in the LSA performed by Hejazi *et al.*<sup>18</sup> are fully borne out by the nonlinear simulations. Indeed, as predicted by the LSA, the reactive situation is always more unstable than the nonreactive one. It is also found that the time at which VF patterns appear in nonlinear simulations is typically above  $t = 100$ , i.e., a time for which the only part of the parameter plane ( $R_b, R_c$ ) to remain stable is that of the monotonic decreasing viscosity profiles obtained for  $2R_b < R_c < 0$ . As discussed in the LSA,

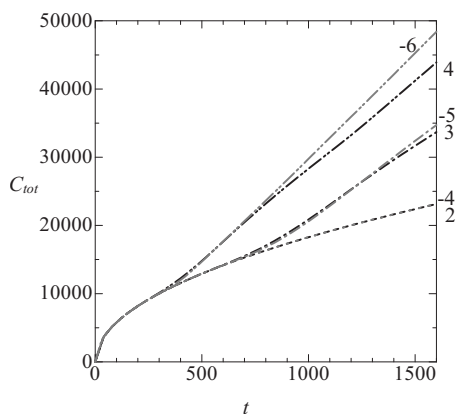


FIG. 17. Temporal evolution of the total amount of product  $C_{tot}$  for  $R_b = -1$  and various values of  $R_c$ . Each curve is the average of three simulations.

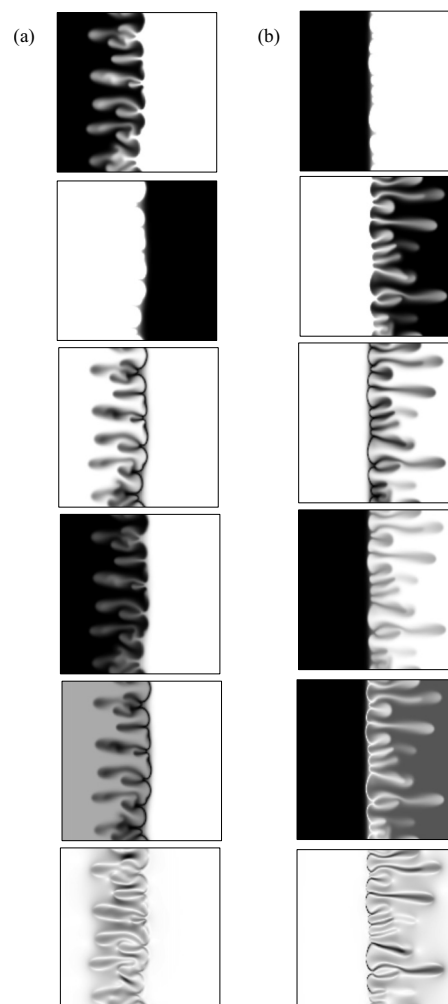


FIG. 18. Concentration of  $A$ ,  $B$ ,  $C$ , and dye  $E$ , viscosity and velocity fields shown from top to bottom for  $R_b = -1$  at time  $t = 2000$  and (a)  $R_c = 4$  and (b)  $R_c = -6$ .

we also find here that systems where fingers develop along the flow are more unstable than when fingers grow against it.

The numerical results for  $R_b > 0$  can be compared with the experimental results by Nagatsu *et al.*<sup>9</sup> using chemical reactions either increasing or decreasing the viscosity, even if their geometries are different (linear in the simulations whereas radial in the experiments). Note that the experiments<sup>9</sup> were done in conditions for which the underlying viscosity profiles remain monotonic ( $0 < R_c < 2R_b$  in the present study). We can quantitatively compare  $L$  and  $FD$  with the equivalent quantities defined in the experiments, respectively, as the length  $l$  of the longest finger and the area occupied by the pattern in a circle whose radius is  $l$ . In the experiment,  $l$  at a later given time is smaller for  $R_c > R_b$  whereas larger for  $R_c < R_b$ . These results are consistent with the numerical results shown for  $L$  in Fig. 9(a). Concerning the finger density, Figs. 11 and 12 in Nagatsu *et al.*<sup>9</sup> showed that the density increases for  $R_c > R_b$  and decreases for  $R_c < R_b$ . These results are consistent with the numerical results shown in Fig. 10 which show the same trend. A difference between the numerical and experimental results is however observed in the finger width. In the experiments (Figs. 5 and

6 in Nagatsu *et al.*<sup>9</sup>), the reaction made the width somewhat larger for  $R_c > R_b$ , whereas smaller for  $R_c < R_b$ . However, the opposite trend is obtained in the present simulation in Figs. 6 and 7. The difference is supposed to be caused by the difference in geometry between the simulation and experiment.

In parallel, numerical simulations also highlight the mechanism proposed by Nagatsu *et al.*<sup>9</sup> to explain their experimental results. These authors hypothesized that the overall reaction rate (production rate of the product) is larger in advanced fingers than in shielded fingers. This was supposed to be due to the fact that the advanced finger has a larger velocity thus has a larger amount of reactant  $A$  provided into the tips of the finger. In the case where the reaction increases the viscosity, the viscosity becomes thus larger and hence the velocity smaller in the advanced finger than in the shielded finger. As a result, the shielding effect is suppressed. An opposite situation occurs when the reaction decreases the viscosity and the shielding effect is enhanced in this case.

In our simulations, the above hypothesis can be tested. In the reference  $R_c = R_b$  nonreactive case [Fig. 12(a)], the velocity is larger in the most advanced finger. When  $R_c > R_b$  with an underlying monotonic viscosity profile like in the experiments of Nagatsu *et al.*<sup>9</sup> [Fig. 12(b)], the concentration of the product is larger and hence the viscosity is larger in the most advanced fingers. The fluid flows therefore preferentially in the neighboring finger where the speed is larger, which leads to suppression of the shielding effect. On the contrary, when  $0 \leq R_c < R_b$  with an underlying monotonic viscosity profile [Fig. 12(d)], the product concentration is larger and the viscosity lower in the most advanced finger. Therefore, the larger velocity is located in the most advanced finger, which results in enhancement of the shielding effect. These various observations indicate that the scenario discussed in the experimental study<sup>9</sup> is fully born out by the present numerical simulations.

## VI. CONCLUSION

Numerical simulations of miscible viscous fingering involving viscosity changes due to an  $A+B \rightarrow C$  chemical reaction have been performed in the case when a solution of reactant  $A$  displaces a solution of reactant  $B$ . The viscosity of the solution is assumed to depend on the concentrations of the chemical species and on two log-mobility ratios  $R_b$  and  $R_c$  measuring the ratio between the viscosity of the  $B$  and  $C$  solutions, respectively, with respect to that of  $A$ . Two types of fingering are obtained depending whether the corresponding nonreactive system of  $A$  displacing  $B$  is viscously stable or not. If the log-mobility ratio  $R_b > 0$ , the reaction modifies the fingering dynamics already present in the nonreactive case. If  $R_b < 0$ , fingering is fully triggered by the reaction provided  $C$  is more ( $R_c > 0$ ) or less viscous ( $R_c < 2R_b < 0$ ) than both reactants. We focus here on conditions for which the diffusion coefficients of all species are the same and the initial reactant concentrations are equal. Moreover, we consider that the Damköhler number  $D_a$  is infinite. We have followed the fingering dynamics by computing among others the spatiotemporal distribution of a dye neutral to the reaction and initially dissolved in the displacing fluid. We quan-

titatively characterized the fingering patterns in terms of the mixing lengths as well as the fingering density FD and the total amount of product  $C_{\text{tot}}$ .

If the nonreactive system is already genuinely unstable ( $R_b > 0$ ), the chemical reaction always destabilizes the system if  $R_c \neq R_b$  as fingering starts then earlier. This effect is further pronounced when the difference  $|R_b - R_c|$  is increasing. Concerning the nonlinear evolution of the fingering, if  $R_c > R_b$ , reverse fingering is privileged, fingers are thinner and denser. In this case, when the underlying viscosity profile is still monotonically increasing, the total mixing length is smaller than in the nonreactive case because the location of largest flow speed switches alternatively from the most advanced finger toward the neighboring one. If  $R_c$  becomes sufficiently large so that the viscosity profile is nonmonotonic with a maximum, the increase in the viscosity jump can compete with this effect and both situations of total mixing lengths either larger or smaller than in the nonreactive case can be observed.

If, on the contrary  $R_c < R_b$  when  $R_b > 0$ , forward fingering is dominant while the finger density decreases as shielding of adjacent fingers is enhanced. The total mixing length is always larger than in the nonreactive case, these effects increasingly monotonically as  $|R_b - R_c|$  is increasing.

If a nonreactive stable situation is considered with  $R_b < 0$ , fingering can be triggered only if the reaction builds up a nonmonotonic viscosity profile which is the case with a maximum or a minimum in viscosity for  $R_c > 0$  and  $R_c < 2R_b < 0$ , respectively. Fingering develops then locally in the region where a less viscous solution pushes a more viscous one. If  $R_c > 0$ , reverse fingering is observed which is of limited extent because of the stable barrier of viscous  $C$  pushing less viscous  $B$  ahead of the reaction zone. This fingering is less effective than the one developing on the leading zone of the viscosity profiles with a minimum ( $R_c < 2R_b < 0$ ) for a same viscosity jump. In this latter case, forward fingering is dominant because fingers extend more easily along the flow than against it.<sup>28</sup> In addition, denser or less dense fingering is observed when  $R_c > 0$  or  $R_c < 2R_b < 0$ , respectively.

Eventually, we note that our results obtained here for the case of an infinite Damköhler number are in good agreement with LSA<sup>18</sup> and experimental results.<sup>9</sup> As other experiments<sup>10</sup> have shown that the properties of fingering can be different for a moderate Damköhler number, an interesting extension of the present work will be to analyze the role of  $D_a$  on the reactive fingering nonlinear dynamics.

We have here assumed that all species diffuse at the same rate. As this is usually not the case, it will be interesting to generalize the present study to cases where the diffusion coefficients can be different. This is likely to enlarge the number of possible dynamics as differential diffusion effects have recently been shown in nonreactive systems to also yield new viscous fingering destabilization scenarios.<sup>29</sup>

## ACKNOWLEDGMENTS

We are grateful to P. M. J. Trevelyan for numerous enlightening discussions. We also thank J. Azaiez, S. H. Hejazi,

R. Maes, and M. Mishra for discussions. Y.N. acknowledges JSPS for a Postdoctoral Fellowship for Research Abroad and for a Grant-in-Aid for Young Scientists (A) (Grant No. 22686020). A.D. thanks Prodex, ESA, the Marie Curie ITN “Multiflow” network, and FNRS for financial support.

- <sup>1</sup>G. M. Homsy, “Viscous fingering in porous media,” *Annu. Rev. Fluid Mech.* **19**, 271 (1987).
- <sup>2</sup>M. Jahoda and V. Hornof, “Concentration profiles of reactant in a viscous finger formed during the interfacially reactive immiscible displacements in porous media,” *Powder Technol.* **110**, 253 (2000).
- <sup>3</sup>Y. Nagatsu and T. Ueda, “Effects of reactant concentrations on reactive miscible viscous fingering,” *AIChE J.* **47**, 1711 (2001).
- <sup>4</sup>Y. Nagatsu and T. Ueda, “Effects of finger-growth velocity on reactive miscible viscous fingering,” *AIChE J.* **49**, 789 (2003).
- <sup>5</sup>Y. Nagatsu and T. Ueda, “Analytical study on effects of finger-growth velocity on reaction characteristics of reactive miscible viscous fingering by using a convection-diffusion-reaction model,” *Chem. Eng. Sci.* **59**, 3817 (2004).
- <sup>6</sup>Y. Nagatsu, T. Ogawa, Y. Kato, and Y. Tada, “Investigation of reacting flow fields in miscible viscous fingering by a novel experimental method,” *AIChE J.* **55**, 563 (2009).
- <sup>7</sup>J. Fernandez and G. M. Homsy, “Viscous fingering with chemical reaction: Effect of in-situ production of surfactants,” *J. Fluid Mech.* **480**, 267 (2003).
- <sup>8</sup>Y. Nagatsu, S. K. Bae, Y. Kato, and Y. Tada, “Miscible viscous fingering with a chemical reaction involving precipitation,” *Phys. Rev. E* **77**, 067302 (2008).
- <sup>9</sup>Y. Nagatsu, K. Matsuda, Y. Kato, and Y. Tada, “Experimental study on miscible viscous fingering involving viscosity changes induced by variations in chemical species concentrations due to chemical reactions,” *J. Fluid Mech.* **571**, 475 (2007).
- <sup>10</sup>Y. Nagatsu, Y. Kondo, Y. Kato, and Y. Tada, “Effects of moderate Damköhler number on miscible viscous fingering involving viscosity decrease due to a chemical reaction,” *J. Fluid Mech.* **625**, 97 (2009a).
- <sup>11</sup>T. Podgorski, M. C. Sostarec, S. Zorman, and A. Belmonte, “Fingering instabilities of a reactive micellar interface,” *Phys. Rev. E* **76**, 016202 (2007).
- <sup>12</sup>T. Gérard and A. De Wit, “Miscible viscous fingering induced by a simple  $A+B \rightarrow C$  chemical reaction,” *Phys. Rev. E* **79**, 016308 (2009).
- <sup>13</sup>A. De Wit and G. M. Homsy, “Viscous fingering in reaction-diffusion systems,” *J. Chem. Phys.* **110**, 8663 (1999).
- <sup>14</sup>A. De Wit and G. M. Homsy, “Nonlinear interactions of chemical reactions and viscous fingering in porous media,” *Phys. Fluids* **11**, 949 (1999b).
- <sup>15</sup>K. Ghesmat and J. Azaiez, “Miscible displacements of reactive and anisotropic dispersive flows in porous media,” *Transp. Porous Media* **77**, 489 (2009).
- <sup>16</sup>S. Swernath and S. Pushpavanam, “Viscous fingering in a horizontal flow through a porous medium induced by chemical reactions under isothermal and adiabatic conditions,” *J. Chem. Phys.* **127**, 204701 (2007).
- <sup>17</sup>S. Swernath and S. Pushpavanam, “Instability of a vertical chemical front: Effect of viscosity and density varying with concentration,” *Phys. Fluids* **20**, 012101 (2008).
- <sup>18</sup>S. H. Hejazi, P. M. J. Trevelyan, J. Azaiez, and A. De Wit, “Viscous fingering of a miscible reactive  $A+B \rightarrow C$  interface: A linear stability analysis,” *J. Fluid Mech.* **652**, 501 (2010).
- <sup>19</sup>S. H. Hejazi and J. Azaiez, “Non-linear interactions of dynamics reactive interface in porous media,” *Chem. Eng. Sci.* **65**, 938 (2010).
- <sup>20</sup>C. T. Tan and G. M. Homsy, “Stability of miscible displacements in porous media: Rectilinear flow,” *Phys. Fluids* **29**, 3549 (1986).
- <sup>21</sup>T. Michioka and S. Komori, “Large-eddy simulation of a turbulent reacting liquid flow,” *AIChE J.* **50**, 2705 (2004).
- <sup>22</sup>C. T. Tan and G. M. Homsy, “Simulation of nonlinear viscous fingering in miscible displacement,” *Phys. Fluids* **31**, 1330 (1988).
- <sup>23</sup>O. Manickam and G. M. Homsy, “Stability of miscible displacements in porous media with non-monotonic profiles,” *Phys. Fluids* **5**, 1356 (1993).
- <sup>24</sup>O. Manickam and G. M. Homsy, “Simulation of viscous fingering in miscible displacements with non-monotonic viscosity profiles,” *Phys. Fluids* **6**, 95 (1994).
- <sup>25</sup>D. Loggia, D. Salin, and Y. C. Yortsos, “The effect of dispersion on the stability of non-monotonic mobility profiles in porous media,” *Phys. Fluids* **10**, 747 (1998).
- <sup>26</sup>D. Schafroth, N. Goyal, and E. Meiburg, “Miscible displacements in Hele-Shaw cells: Non-monotonic viscosity profiles,” *Eur. J. Mech. B/Fluids* **26**, 444 (2007).
- <sup>27</sup>L. Rongy, P. M. J. Trevelyan, and A. De Wit, “Dynamics of  $A+B \rightarrow C$  reaction fronts in the presence of buoyancy-driven convection,” *Phys. Rev. Lett.* **101**, 084503 (2008).
- <sup>28</sup>M. Mishra, M. Martin, and A. De Wit, “Differences in miscible viscous fingering of finite width slices with positive or negative log-mobility ratio,” *Phys. Rev. E* **78**, 066306 (2008).
- <sup>29</sup>M. Mishra, P. M. J. Trevelyan, C. Almarcha, and A. De Wit, “Influence of double diffusive effects on miscible viscous fingering,” *Phys. Rev. Lett.* **105**, 204501 (2010).